P66Shc Mediates SUMO2-induced Endothelial Dysfunction

Jitendra Kumar[1], Shravan K Uppulapu[1], Sujata Kumari[1], Kanika Sharma[2], William Paradee[3], Ravi Prakash Yadav[4], Vikas Kumar[2], and Santosh Kumar[1]

[1] Department of Internal Medicine, Division of Cardiovascular Medicine, University of Iowa, Iowa City, IA, 52242

[2]Department of Genetics, Cell Biology and Anatomy, University of Nebraska Medical Center, Omaha, NE, 68198

[3]Genome Editing Core Facility, University of Iowa, Iowa City, IA, 52242

[4]Regional Institute of Education-NCERT, Mysore, Karnataka, 570006, India

Corresponding author:
Santosh Kumar
25 South Grand Avenue,
ML B191
University of Iowa,
Iowa City, IA-52242
Phone: 31933592238
Email: santosh-kumar@uiowa.edu

Author Contributions: JK, SKU, SK (Sujata Kumari), KS, SK1 performed studies, analyzed data, and prepared figures; WP and RPY contributed to reagent generation and validation; VK and SK1 analyzed data, prepared figures and wrote manuscript.

Competing Interest Statement: The authors have declared that no conflicts of interest exist.

Summary

Sumoylation is a post-translational modification that can regulate different physiological functions. Increased sumoylation, specifically conjugation of SUMO2/3 (small ubiquitin like modifier 2/3), is detrimental to vascular health. However, the molecular mechanism mediating this effect is poorly understood. Here, we demonstrate that SUMO2 modifies p66Shc, which impairs endothelial function. Using multiple approaches, we show that p66Shc is a direct target of SUMO2. Mass spectrometry identified that SUMO2 modified lysine-81 in the unique collagen homology-2 domain of p66Shc. SUMO2ylation of p66Shc increased phosphorylation at serine-36, causing it to translocate to the mitochondria. Notably, sumoylation-deficient p66Shc (p66ShcK81R) was resistant to SUMO2-induced p66ShcS36 phosphorylation and mitochondrial translocation. Ingenuity pathway analysis showed that majority of effects of p66Shc SUMO2ylation were mediated via p66ShcK81. Finally, p66ShcK81R knockin mice were resistant to SUMO2-induced endothelial dysfunction. Collectively, our work uncovers a posttranslational modification of redox protein p66Shc and identifies SUMO2-p66Shc signaling as a regulator of vascular endothelial function.

Keywords: Sumoylation, endothelial function, p66Shc, SUMO

Introduction

Endothelial cells play an important role in regulating vascular health. One of the primary functions of endothelial cells is to maintain vascular tone and regulate blood flow in response to physiological changes. In the context of disease, endothelial cells either fail to produce enough nitric oxide (NO) or the available NO is quenched by reactive oxygen species (ROS). Consequently, this leads to endothelial dysfunction (ED), characterized by the reduced availability of NO and impaired vasorelaxation [1]. ED is associated with various conditions such as diabetes, hyperlipidemia, hyperglycemia, obesity, and aging [2]. There is a strong correlation between ED and atherosclerotic changes in vessel walls [3]. Therefore, ED is one of the prime targets to prevent pathologies including myocardial infarction and stroke.

Sumoylation is a dynamic post-translational modification involved in many pathologies including vascular disease [4]. Increased sumoylation promotes ED and subsequent development of atherosclerosis [5,6]. Sumoylation occurs by conjugation of **s**mall **u**biquitin-like **mo**difier**s** (SUMOs) to the lysine moiety of the target protein, which may change its fate and/or function. SUMO conjugation is predicted to occur at a specific motif, ΨKXE, where Ψ represents an aliphatic-branched amino acid, X a random amino acid, and E glutamic acid, although other non-canonical sumoylation sites have also been reported [4,7,8]. There are four SUMO isoforms (SUMO1, SUMO2, SUMO3 and SUMO4) and among them SUMO2 is the most abundantly expressed. Unlike SUMO1 and SUMO3, genetic deletion of SUMO2 is embryonically lethal [9,10]. While sumoylation is known to promote cardiovascular diseases, the effect of SUMO isoforms on the vasculature is not well studied. Recently, we reported that endothelial-specific overexpression of SUMO2 impairs vascular endothelial function in mice [11]. However, the molecular mechanism mediating the endothelial effects of SUMO2 are not known.

p66Shc is a member of the ShcA family of adaptor proteins. Among the ShcA protein family (p66Shc, p52Shc, and p46Shc), p66Shc is the largest protein due to an additional collagen homology domain (CH2) at its N-terminus. Posttranslational modifications in the CH2 domain regulate the oxidative function of p66Shc [12-15]; whereas phosphorylation in the CH1 domain leads to mitogenic signaling [16,17]. p66Shc is abundantly expressed in endothelium and mediates ED due to hyperlipidemia, hyperglycemia, and aging [18]. Correspondingly, mice with a genetic

deletion of p66Shc have a longer life span and are protected against ED due to metabolic disorders [19,20]. Here, we examined whether p66Shc mediates SUMO2-induced ED and oxidative stress. Using multiple techniques, we show that SUMO2 directly modifies p66Shc at lysine-81 in its CH2 domain, which is essential for SUMO2-induced ROS production and ED. Thus, our study uncovers a previously unknown posttranslational modification that regulates p66Shc function in the endothelium and defines a novel molecular mechanism by which increased SUMO2ylation induces ROS, leading to vascular ED.

Results

P66Shc mediates SUMO2-induced ROS production and inflammation in endothelial cells. To address whether p66Shc mediates SUMO2-induced ROS production, we overexpressed SUMO2 in human umbilical vein endothelial cells (HUVECs) with and without knockdown of p66Shc. As expected, overexpression of SUMO2 led to a robust increase in levels of ROS (Fig. 1A and B). This SUMO2-induced increase in ROS was significantly blunted in HUVECs with p66Shc knockdown (Fig. 1A and C). Increased ROS promotes inflammation [21], therefore, we examined endothelial inflammation when SUMO2 was overexpressed in HUVECs. Indeed, SUMO2 overexpression in HUVECs showed a significant increase in ICAM1 expression (Fig. S1). Further, we asked whether p66Shc mediates SUMO2-induced inflammation. In HUVECs, knockdown of p66Shc abrogated SUMO2-induced increases in ICAM1 levels (Fig. 1 D and E). Together, these findings suggest that p66Shc mediates the effects of SUMO2 on endothelial cells.

p66Shc is directly modified by SUMO2. We next asked if p66Shc is a direct target for SUMO2. We overexpressed p66Shc in HEK-293 cells with and without SUMO2. Immunoprecipitation of p66Shc showed many slower migrating protein bands when SUMO2 and p66Shc were co-expressed, suggesting that p66Shc may be SUMO2ylated (Fig. 2A). To confirm that the slower migrating bands were due to sumoylation, we overexpressed SUMO-ligase (Ubc9) to facilitate sumoylation, and a deSUMOylating enzyme (SENP1) which removes SUMO proteins. Overexpression of Ubc9 increased the signal of slower migrating bands whereas SENP1 reduced the signal suggesting the slower migrating bands were due to

sumoylation (Fig. 2B). Next, we asked whether the SUMO2-p66Shc interaction exists in endothelial cells by overexpressing SUMO2 and p66Shc in HUVECs. Immunoprecipitation of flag-tagged p66Shc revealed sumoylation (Fig. 2C) which consistently increased in intensity with increasing SUMO2 expression (Fig. S2). To verify that p66Shc undergoes SUMO2ylation in HUVECs we treated cells with a pharmacological inhibitor of sumoylation (anacardic acid). This reduced sumoylation of p66Shc (Fig. 2D), demonstrating that indeed p66Shc undergoes SUMO2ylation in endothelial cells. We also performed an *in vitro* sumoylation of p66Shc using recombinant His-tagged p66Shc protein and a commercially available kit (Enzo, Farmingdale, NY), which showed that recombinant p66Shc is modified by SUMO2 (Fig. 2E). Collectively, these findings indicate that p66Shc is a direct target of SUMO2.

SUMO2 modifies p66Shc via lysine-81. The CH2 domain of p66Shc is highly conserved and involved in oxidative function of p66Shc. Within this region are several conserved lysine residues. Among these is lysine 81, which is part of the ΨKXE motif required for sumoylation (Fig. 3A) Therefore, to examine if K81 is sumoylated, we took advantage of SUMO2ylated recombinant p66Shc and resolved it on SDS-PAGE. Based on the approximate location of modified protein bands seen in immunoblotting, we cut out the gel piece and subjected it to mass spectrometry analysis (Fig. S3). This identified that lysine-81 (K81) in p66Shc was SUMO2ylated, identified as lysine conjugated with the QTGG motif present at c-terminal of SUMO2 (Fig. 3B). To confirm that SUMO2 modifies p66Shc at K81, we mutated this residue to Arginine (p66ShcK81R) and overexpressed it in HEK-293 cells with SUMO2 to determine if sumoylation still occurred. Immunoprecipitation showed that p66ShcK81R is resistant to SUMO2ylation, whereas it still occurred with the wild-type (WT) form (Fig. 3C). Similar results were also observed in HUVECs (Fig. 3D). We next performed an *in vitro* SUMO2ylation of recombinant p66ShcWT and p66ShcK81R. As anticipated, immunoblotting showed that, unlike p66ShcWT, p66ShcK81R is resistant to SUMO2ylation (Fig. 3E). Thus, our findings demonstrate that SUMO2 modifies p66Shc at K81.

SUMO2 promotes serine36 phosphorylation and mitochondrial translocation of p66Shc. In response to pro-oxidant stimuli, p66Shc becomes phosphorylated at serine36 (S36) and translocates to mitochondria. Once there it oxidizes cytochrome C to produce ROS [22,23], which is

a central mechanism to activate the oxidative function of p66Shc. Since the K81 and S36 residues of p66Shc are both present in its conserved CH2 domain, we asked whether promoting SUMO2ylation also facilitates phosphorylation of the S36 residue of p66Shc. In HEK-293 cells as well as in HUVECs, we noted increased levels of p66ShcS36 phosphorylation when SUMO2 and p66Shc were co-expressed (Fig. 4A-D). To determine whether SUMO2-induced S36 phosphorylation is mediated via K81 sumoylation, we evaluated p66ShcS36 phosphorylation in HUVECs overexpressing p66ShcK81R and SUMO2. SUMO2 overexpression significantly increased S36 phosphorylation in cells expressing p66ShcWT whereas cells expressing p66ShcK81R were resistant to this increase (Fig. 4E and F). As p66ShcS36 phosphorylation increases p66Shc level in mitochondria, we evaluated whether SUMO2 affects mitochondrial levels of p66Shc. Levels of p66Shc in the mitochondria of HUVECs increased in a dose-dependent manner upon SUMO2 overexpression (Fig. 5A and B). However, mitochondrial expression of p66Shc was significantly lower in HUVECs expressing p66ShcK81R relative to p66ShcWT (Fig. 5C and D). We also verified that SUMO2-dependent regulation of p66ShcS36 phosphorylation is an upstream event by evaluating the effect of SUMO2 on p66Shc binding to prolyl isomerase (PIN1) and noted that SUMO2 does not affect p66Shc-PIN1 association (Fig. S4).

Mitochondrial p66Shc is not SUMO2ylated. Since promoting sumoylation increased mitochondrial levels of p66Shc, we examined whether sumoylated p66Shc translocates into mitochondria. To determine this, we generated an antibody using a commercial source (YenZym, CA) to detect sumoylated-p66Shc. This antibody was validated for its specificity in detecting sumoylated p66Shc in HUVECs (Fig. S5). We then assessed sumoylated-p66Shc in mitochondria by overexpressing SUMO2 with p66Shc in HUVECS. Overexpression of SUMO2 with p66Shc showed SUMO2ylated p66Shc in whole cell lysate, but not in the mitochondrial fraction despite the robust increase in mitochondrial levels of p66Shc that were induced by SUMO2 (Fig. 5E). Overall, these findings suggest that even though SUMO2 modification predisposes p66Shc for S36 phosphorylation and mitochondrial translocation, mitochondrial p66Shc is not sumoylated.

Mice expressing non-sumoylatable p66ShcK81R are protected against SUMO2-induced ED. To examine whether SUMO2ylation of p66ShcK81 affects endothelial control of vascular

tone, we generated a mouse model with endogenous p66Shc mutated to p66ShcK81R (p66ShcK81R knockin mice). Using the CRISPR-Cas9 technique, a mutation was induced that caused arginine to be synthesized in place of lysine at position 81 in p66Shc (Fig. 6 A and B). The p66ShcK81R knockin mice had no alterations in the expression of p66Shc in the aorta (Fig. S6). To examine the effect of SUMO2 on endothelial function in these mice, we used adenoviruses to express SUMO2 in aortic rings from WT and p66ShcK81R knockin mice (Fig. 6 C and D). Subsequently, the aortic rings were evaluated for endothelium-dependent relaxation (induced by acetylcholine) and endothelium-independent relaxation (induced by sodium nitroprusside). In aortic rings from WT mice, endothelium-dependent relaxation was significantly delayed by SUMO2 overexpression (Fig. 6E) whereas it was unchanged in p66ShcK81R mice (Fig. 6F). In contrast, endothelium-independent relaxation was not affected by SUMO2 overexpression (Fig. 6 G and H). This suggests that the effect of SUMO2 on endothelial function is primarily mediated via p66ShcK81. Collectively, our study shows that p66Shc mediates the effects of SUMO2 on vascular tone.

Endothelial effects of SUMO2-p66Shc is mediated via p66ShcK81. Given that SUMO2 modifies p66Shc at K81 and causes endothelial dysfunction, we next asked how p66ShcK81-SUMO2 affects endothelial cells. We performed global proteomics profiling of HUVECs overexpressing SUMO2 and p66ShcWT or p66ShcK81R using mass spectrometry (Fig. S7). Comparative analysis of protein expression was performed against control (HUVECs infected with an equal number of adenovirsues expressing LacZ). Compared to control, almost 400 proteins were significantly upregulated/downregulated in cells expressing SUMO2 and p66ShcWT and a majority of them were not significantly changed in cells expressing SUMO2 and p66ShcK81R. To gain insights into the biological significance of these changes, we preformed Ingenuity Pathway Analysis (IPA) to identify signaling pathways relevant to cardiovascular disease and cell signaling. Multiple pathways were significantly affected by the presence of SUMO2-p66Shc (Fig. 7). A majority of pathways were downregulated by SUMO2-p66Shc, and a few were upregulated, however these changes were normalized in cells expressing p66ShcK81R. We expanded this analysis to include all pathways in the IPA application. This showed additional pathways that were downregulated and upregulated in SUMO2-p66ShcWT expressing cells. All of these pathways were normalized in SUMO2-p66ShcK81R expressing

cells, except for *cardiac hypertrophy* and *Rho-GTPase signaling*, which were only partially rescued. Interestingly, in endothelial cells expressing p66ShcK81R the *cardiac hypertrophy* pathway was downregulated whereas the *C-type lectin receptors* and *Myelination signaling* pathways were upregulated (Fig. S8). This nuanced analysis provides a comprehensive understanding of the intricate network of pathways affected by SUMO2 modification of p66ShcK81 on p66Shc and highlights the specific impact of the p66ShcK81R mutant on these cellular processes.

Discussion

Although SUMO2 and p66Shc are expressed in endothelium and are associated with ED, the mechanisms by which this occurs are unclear. Here we identified SUMO2 modification of p66Shc as a novel molecular signal regulating vascular endothelial function. SUMO2 modifies p66Shc at K81, which increases phosphorylation of p66Shc at S36, resulting in its translocation to the mitochondria. These steps are critical for p66Shc-dependent ROS production. Notably, this phenomenon was evident in non-endothelial cells as well, suggesting that SUMO2-p66Shc may also regulate other physiologic functions. Mice expressing a non-sumoylatable form of p66Shc (p66ShcK81R KI) were protected against SUMO2-induced ED, which further supports the role of SUMO2-p66ShcK81 in regulating endothelium function.

Multiple studies suggest that sumoylation promotes ED [24]. Preventing sumoylation by downregulating the SUMO ligases, Ubc9 (E2 ligase) and PIAS1 (E3 ligase), rescued oxidative stress and advanced glycation end product-mediated endothelial inflammation and dysfunction [25]. Conversely, partial genetic deletion of the de-sumoylation enzyme, sentrin/SUMO-specific protease 2 (SENP2), significantly increased endothelial apoptosis, inflammation, and dysfunction, which promoted atherosclerotic plaque formation [5,6]. However, the isoform-specific effects of SUMOs on endothelial function have not been well studied. We previously reported that endothelial expression of SUMO2 impairs vasorelaxation [11]. By showing that p66Shc mediates the endothelial effects of SUMO2, this study explains the prior findings that the effects of SUMO2 on vasculature are likely mediated by p66Shc.

The adapter protein p66Shc mediates receptor tyrosine kinase signaling in a variety of cell types. Among them, the effects of p66Shc on endothelial cells are well studied and pronounced [18]. In particular, endothelial function in mice with genetic deletion of p66Shc are protected against a variety of stimuli such as diabetes, aging, and hyperlipidemia [19,20,26]. p66Shc produces ROS by oxidation of cytochrome C in the mitochondria as well as by activating Rac1 [13,23]. Phosphorylation at S36 in the CH2 domain of p66Shc is one of the earliest discovered posttranslational modifications that govern its oxidative function [12]. Crosstalk among different posttranslational modifications including phosphorylation, acetylation, and sumoylation is well known [27-30]. Our finding that SUMO2 increases S36 phosphorylation in p66Shc (Fig. 4) suggests the existence of such a crosstalk in regulating the oxidative function of p66Shc. The molecular weight of the phosphorylated p66ShcS36 protein band (close to 70kD) suggests that the pool of SUMO2-induced phosphorylated p66ShcS36 is not sumoylated. Therefore, it is likely that K81-SUMOylated and S36-phosphorylated forms of p66Shc coexist in the same pool of protein, but that p66Shc is not SUMOylated and phosphorylated at the same time. Future studies will be needed to establish the hierarchy of this phenomena.

SUMO2-induced increases in mitochondrial levels of p66Shc were dependent on its phosphorylation at S36, as the absence of SUMO2ylation due to expression of p66ShcK81R prevented S36 phosphorylation. SUMO2 did not affect p66Shc-PIN1 binding (Fig. S4), a step that is critical for isomerization and mitochondrial translocation of p66Shc [12]. Also, SUMO2ylated p66Shc is not present in mitochondria (Fig. 5E). These findings are in line with that noted with p66ShcS36 phosphorylation [12], which suggest that a post-translationally modified form of p66Shc does not translocate to mitochondria; instead it is the downstream modifications that likely facilitate this process.

Based on mass spectrometry analysis and *in vitro* sumoylation of recombinant p66Shc, it appears that p66ShcK81 is a primary target of SUMO2. However, the multiple protein bands higher than 66kD that were present in the immunoprecipitation assay suggest the possibility that additional sumoylation sites are present in p66Shc. Technical challenges limited our ability to determine the nature of these protein bands. Yet, in silico analysis using an available sumoylation prediction tool (Cuckoo workgroup) indicates 3 possible sumoylation motifs present in p66Shc, namely

K81, K462, and K582, which can non-specifically be modified by SUMO1/2/3/4. Immunoblot with p66Shc-SUMO2 antibody also suggests that p66Shc is SUMO2ylated at lysine other than K81 (Fig. S5). Importantly, among the possible sumoylation motifs only K81 is present in the CH2 domain, which is unique structural feature of p66Shc (i.e., not present in other isoforms: p52Shc and p46Shc) that has a regulatory effect on its function. Therefore, even though other lysines are sumoylated, it is likely that the effect of p66Shc-sumoylation is mediated through the K81 modification and has also been supported by proteomics analysis.

To understand the mechanism by which SUMO2-p66ShcK81 regulates endothelial cells, we performed global proteomic analysis. Among several downregulated pathways, Rho-GTPase was highly affected by SUMO2-p66Shc (Fig. 7). Shc isoforms differentially participate in Rho-GTPase signaling: p66Shc binds to the RhoA/B/C family of proteins while p52Shc interacts with Ras and Rac [31]. Interestingly, HUVECs expressing p66ShcWT showed an upregulation of RhoGDI signaling and downregulation of Rho-GTPase. RhoGDI negatively regulates Rho-GTPase signaling by binding Rho-GTPase and inhibiting its membrane translocation[32]. Although not investigated here, upregulation of Rho-GDI by p66Shc sumoylation could be another possible pathway by which p66Shc regulates Rho-GTPase signaling. Given the diversity of Rho family GTPases and their complexity, it is difficult to pinpoint the specific pathway being affected by SUMO2-p66Shc; however, Rho-GTPase downregulation was mitigated and Rho-GDI signaling was upregulated in cells expressing SUMO2-p66ShcK81R, suggesting the possible involvement of p66ShcK81 in Rho-GTPase signaling. Additionally, it is noteworthy that cells expressing p66ShcK81R also elicit responses that are not significantly affected by SUMO2-p66Shc, such as activation of C-type lectin receptors and myelination signaling (Fig. S8). Both C-type lectin receptors and myelination signaling are known be active in endothelial cells[33,34]. Although, their relationship with p66ShcK81R will require future studies, preventing p66ShcK81 modification may activate these non-canonical pathways in p66Shc signaling.

One of the limitations of this study is that we did not perform gain-of-function experiments to ascertain if SUMO2-modified p66ShcK81 regulates p66Shc function *in vivo*, which is technically too challenging. Prior studies have shown that K81 of p66Shc gets acetylated [14] and that a specific lysine can get sumoylated as well as acetylated [29]. Although p66ShcK81R disrupts

acetylation and sumoylation that occurs from acetyl transferase and SUMOylating enzymes, it is possible that the same lysine is sumoylated and acetylated in a context dependent manner. Importantly, the extent of post translational modification is so small that a competition between acetylation and sumoylation for the same target residue is highly unlikely. The fact that p66ShcK81R KI mice are protected against SUMO2-induced ED supports the hypothesis that p66ShcK81 mediates the endothelial effects of SUMO2.

Collectively, our study identified p66Shc SUMO2ylation as a unique cellular signaling mechanism specifically regulating vascular endothelial function. As such, this signaling mechanism may also affect advanced pathologies such as atherosclerosis, where both increased SUMOylation and expression of p66Shc has been reported. Nevertheless, given its potential to regulate endothelial function, SUMO2ylation of p66Shc presents a novel therapeutic target for pathologies associated with ED.

Materials and Methods

Animals: All experimental animal procedures were approved by the Institutional Animal Care and Use Committee at the University of Iowa and conformed to the Guide for the Care and Use of Laboratory Animals published by the National Institutes of Health. Wild-type mice (C57BL/6) were procured from Jackson lab. The p66ShcK81R knockin mice were generated with the help of Genome Editing Core Facility, University of Iowa, Iowa City. Using a CRISPR-Cas9 technique, a mutation was introduced in the embryos from C57BL/6J mice and the embryos were implanted to pseudo-pregnant females. Founders were identified by PCR genotyping and Sanger sequencing. Subsequently mice were inbred to generate homozygous p66ShcK81R knockin mice.

Genotyping protocol for p66ShcK81R: DNA was isolated from ear punches of mice using a commercially available DNA isolation kit (NucleoSpin Tissue DNA, Machery-Nagel GmbH & Co.). Polymerase chain amplification (PCR) was performed to amplify the DNA sequence around the knockin position using Phusion high-fidelity DNA polymerase master mixture reaction (NEB); forward primer (5’- CTT CGG AAT GAG TCT CTG TCA TC-3’) and reverse primer (5’- ACC CGA ACC AAG TAG GAA ACG-3’). The reaction mixture was pre-heated at

70°C for 2 min followed by initial denaturation at 98°C for 2 min, then 35 cycles at 98°C for 20s, 62°C for 30s, 72°C for 40 sec, and a final extension at 72°C for 5min. PCR amplified products were digested with ApaI enzyme at 37°C for 2.5 h. Agarose gel electrophoresis was performed to determine the amplification and digestion pattern of the amplicon. Mice identified by genome sequencing were used as a positive control.

Cell culture: Human umbilical vein endothelial cells (HUVECs) were purchased from Promocell (Heidelberg, Germany) and Lonza (Walkersville, MD) and were cultured in endothelial growth medium-2 from Promocell and Lonza. HEK 293 cells were cultured in DMEM (Gibco) supplemented with 10% fetal bovine serum (Thermo), and 1% Pen Strep (penicillin 10,000 Units/mL and 10,000 ug/mL streptomycin; Gibco).

Reagents: Primary antibodies: Monoclonal Flag (Catalog no. F1804, Sigma, MO); Monoclonal GAPDH (Catalog no. 2118S, Cell Signaling Technology, MA); monoclonal Senp1 (Catalog no. sc- 271360, Santa Cruz Biotechnology, TX); Monoclonal HA (Catalog no. 3724s Cell Signaling Technology); Monoclonal His-tag (Catalog no. 2366S Cell Signaling Technology); Polyclonal Phospho-p66Shc (Catalog no. Ab267413 Abcam, MA); Monoclonal PIN1 (Catalog no. MAB2294, R&D, MN); SUMO2/3 (Catalog no. 633306, Sigma and Catalog no. 4971, Cell Signaling Technologies); Monoclonal Ubc9 (D26F2) (Catalog no. XP 4786s, Cell Signaling Technology); PhosphoDetect Anti-Shc/p66 (Catalog no. 566807, Millipore Sigma, MO); Cox IV (3E11) (Catalog no. 4850S, Cell Signaling Technology),\; sumoylation kit (Enzo Life Sciences, NY).

Secondary antibodies: polyclonal IR-dye 800 Rb (Catalog no. ab216773, Abcam); polyclonal IR-dye 680 (Catalog no. ab216776, Abcam); anti-rabbit IgG HRP linked (Catalog no. 7074S, Cell Signaling Technology); anti-mouse IgG HRP linked (Catalog no. 7076S, Cell Signaling Technology).

Plasmids: We generated a new construct of p66Shc (human) with a Flag tag (DYKDDDDK) at the N-terminus (Flag-p66Shc) in the pcDNA3 backbone. FNpCDNA3 was a gift from Dr. Robert Oshima (Addgene plasmid # 45346). We also generated HA-tagged (MYPYDVPDYA) SUMO2 (Human) in the same backbone. Successful cloning was verified by DNA sequencing. FLAG-SENP1 (Addgene plasmid # 17357) [35] and Ubc9 (Addgene plasmid # 20082) [36] was a gift from Dr. Edward Yeh.

Adenoviruses: Adenoviruses of Flag-p66ShcWT, Flag-p66ShcK81R, and HA-SUMO2 were generated with the help of Viral Vector Core facility, University of Iowa. Target sequences were cloned to a shuttle vector. For adenoviral expression, Flag-p66ShcWT, Flag-p66ShcK81R, and HA-SUMO2 were cloned into a shuttle vector plasmid (G0688pacAd5CMV) provided by the Viral Vector Core facility. Constructs were verified for proper inserts by digestion followed by Sanger sequencing. Further processing was supported by the Viral Vector Core facility.

Mutagenesis of p66Shc: To create p66ShcK81R, we performed site-directed mutagenesis on Flag-p66Shc to induce an AAG to AGA mutation. The following primers were used: forward 5'-cctggctcccctctagaccctgggcgcc-3' and reverse 5'-ggcgcccagggtctagaggggagccagg-3'. Successful mutagenesis was verified by DNA sequencing.

Adenoviral expression: An optimum volume of viral stock was added to the cells with growth medium. We used 1:100 MOI in most of the experiments. Specific MOI is described in the figures Cells were analyzed almost 40 h of infection.

Plasmid and siRNA transfection: For plasmids transfection, Lipofectamine 2000 (Invitrogen, MA) was used as per the manufacturer instructions. For 1 μg of plasmid, we used 2 μl lipofectamine. p66Shc-specific siRNAs (custom made) and a non-specific control siRNA were purchased from Invitrogen. An appropriate amount of siRNA was incubated with Lipofectamine2000 (Invitrogen) at room temperature for 20 min before adding to cells prepared with OPTI-MEM media (Invitrogen). Four hours later the media was replaced with fresh endothelial growth media and cells were cultured for an additional 48 hours.

Recombinant protein expression and purification: Purified recombinant protein was synthesized as published earlier with slight modification [37]. DNA sequences coding His-p66ShcWT and His-p66ShcK81R proteins were PCR-amplified from Flag-p66ShcWT and Flag-p66ShcK81R plasmids. PCR amplified His-p66ShcWT and His-p66ShcK81R were cloned into the pET 21a expression vector. Sanger sequencing confirmed the presence of the insert. Sequenced plasmids were transformed into Rosetta 2 (de3) cells and inoculated into 50 ml of LB broth supplemented with 50 μl ampicillin (100μg/ml) and 50 μl chloramphenicol (34μg/ml) antibiotics. The cells were then incubated overnight at 37°C at 250 rpm for growth. For secondary inoculum, 10 ml of the primary culture was inoculated into 1L of 2xYT media (Yeast-Tryptone) and incubated at 37°C until the O.D. reached 0.6 at 600nm. Cultures were then cooled

at 2-8°C for a minimum of 20 minutes, followed by 5 minutes at room temperature. Induction of the culture was done using 0.250 mM IPTG, and the incubation continued at 16°C, 200 rpm overnight. The culture was pelleted down by centrifugation at 4°C. The cell pellets were sonicated on ice (five 30s pulses). The lysed sample was centrifuged at 18000 rpm for one hour at 4°C. The supernatant was collected and passed through a pre-packed, pre-equilibrated Ni-NTA resin column for protein purification. Western blotting confirmed the presence of the target protein.

Mass spectrometry for sumoylation and Data Analysis: Recombinant p66Shc was sumoylated with a commercially available sumoylation kit (Enzo Life Sciences). Sumoylated protein was resolved by SDS-PAGE. Gels were stained with mass spectrometry compatible silver stain (SilverQuest, Invitrogen). Gel pieces were excised based on the observed SUMOylation signal in the immunoblot of recombinant p66Shc. Gel pieces were de-stained and reduced with 5 µL of 200 mM tris(2-carboxyethyl) phosphine (TCEP) (1 h incubation, 55 ºC) and alkylated with 5 µL of 375 mM iodoacetamide (IAA) (30 min incubation in the dark, room temperature). The protein digestion was carried out using 2.5 µg of trypsin per sample (16 h incubation, 37 ºC). The next day, samples were dried out using a speed vacuum and then desalted with C18 spin columns (Pierce, MA). Clean peptides were dried out again with a speed vacuum and resuspended in 0.1% formic acid, and next analyzed using a high-resolution mass spectrometry nano-LC-MS/MS Tribrid system, Orbitrap Fusion™ Lumos™ coupled with UltiMate 3000 HPLC system (Thermo Fisher Scientific). Peptide identification was performed by searching MS/MS data against the p66Shc protein sequence in Peaks Studio. We detected a missed cleavage at a lysine (K) residue as shown in the figure 3B, which was followed by a QTGG modification with a mass of 343.15 Da. This specific mass shift was consistent with the expected tryptic peptide from sumoylated peptide as shown by other studies [38,39].

Label free quantitative mass spectrometry and data analysis: HUVECs were infected with Ad-HA-SUMO2 znd Ad-Flag-p66ShcWT or Ad-Flag-p66ShcK81R. Samples were lysed in RIPA buffer and protein expression was determined by immunoblotting. Whole cell lysate having 50 µg of protein per sample from six biological replicates per group was taken and detergent was removed by chloroform/methanol extraction, and the protein pellet was re-suspended in 100 mM ammonium bicarbonate and digested with MS-grade trypsin (Pierce) overnight at 37°C following reduction with 10 mM DTT at 56° C for 30 mins and alkylation

using 50 mM iodoacetamide at RT for 25 mins. Peptides were cleaned with PepClean C18 spin columns (Thermo) and were re-suspended in 2% acetonitrile (ACN) and 0.1% formic acid (FA) and 500 ng of each sample was loaded onto trap column Acclaim PepMap 100 75µm x 2 cm C18 LC Columns (Thermo Scientific™) at flow rate of 4 µl/min then separated with a Thermo RSLC Ultimate 3000 (Thermo Scientific™) on a Thermo Easy-Spray PepMap RSLC C18 75 µm x 50 cm C-18 2 µm column (Thermo Scientific™) with a step gradient of 4–25% solvent B (0.1% FA in 80 % ACN) from 10-100 min and 25–45% solvent B for 100–130 min at 300 nL/min and 50oC with a 155 min total run time. Eluted peptides were analyzed by a Thermo Orbitrap Exploris 480 (Thermo Scientific™) mass spectrometer in a data dependent acquisition mode. A survey full scan MS (from m/z 350–1200) was acquired in the Orbitrap with a resolution of 60,000. The Normalized AGC target for MS1 was set as 300% and ion filling time set as 25 ms. The most intense ions with charge state 2-6 were isolated in 3 s cycle and fragmented using HCD fragmentation with 30 % normalized collision energy and detected at a mass resolution of 15,000 at 200 m/z. The AGC target for MS/MS was set as 50% and ion filling time set to auto for 30 s with a 10 ppm mass window. Protein identification was performed by searching MS/MS data against the swiss-prot human protein database using the in house PEAKS X + DB search engine. The search was set up for full tryptic peptides with a maximum of two missed cleavage sites. The precursor mass tolerance threshold was set 10 ppm for and maximum fragment mass error was 0.02 Da. The significance threshold of the ion score was calculated based on a false discovery rate of ≤ 1%. Quantitative data analysis was performed using progenesis QI proteomics 4.2 (Nonlinear Dynamics). Statistical analysis was performed using ANOVA and The Benjamini-Hochberg (BH) method was used to adjust p values for multiple-testing caused false discovery rate. The adjusted $p \leq 0.05$ was considered as significant. Ingenuity pathway analysis was used to identify pathways being affected p66ShcK81 SUMO2ylation.

Whole cell ROS assay by spectrophotometry: HUVECs were plated in clear-bottom black-walled 96 well plates and infected with adenoviruses encoding HA-SUMO2 or control virus encoding LacZ. For ROS detection and quantification, cells were incubated with MitoSOX (2µM, Life Technologies) in EBM2 for 30 min. at 37°C in CO_2 incubator. Following incubation, cells were washed with pre-warmed EBM2 media and maintained at 37°C in a CO_2 incubator for another 30 min. MitoSOX fluorescence was measured at 396/610 nm using a plate reader. Each well was measured at 4 different points at the 1 mm distance and the mean was considered as

final reading of that well. Values were normalized against the background fluorescence. We excluded the first and last row in each plate.

Immunoprecipitation: Protein lysate was pre-cleared using Sepharose beads for 2 hours at 4°C on the rocker. The supernatant was collected and incubated with the specified antibody (1 ug of antibody/mg protein) and Sepharose beads overnight at 4°C. Sepharose beads were washed 8 times with ice cold lysis buffer (1 ml each wash). After that the beads were boiled for 5 min at 95°C and subjected to SDS-PAGE.

Immunoblotting: Cells or tissues were washed with PBS and lysed in an appropriate amount of protein lysis buffer (TritonX100 -1%, Tris 7.4 -50mM, EDTA -5mM, NaCl -150mM, and glycerol -5%) containing Protease Inhibitor Cocktail (Roche). We used Phosphatase Inhibitor Cocktail (Millipore) and de-sumoylation inhibitor N-ethylmaleimide (20 mM) in the lysis buffer where appropriate. Cell lysis was performed by repeated freeze thaw followed by sonication for 25 sec (5 sec on, 2 sec off, and 20% amp). Homogenate was centrifuged at 13000g for 20 mins at 4°C, supernatant was used for protein quantification.

We used approximately 30 ug of protein lysates. Cell lysate was mixed with protein loading dye and boiled at 95 ºC for 5 min. Following brief centrifugation, lysates were loaded onto acrylamide gel for SDS-PAGE. Protein was transferred to a nitrocellulose membrane. Membranes were treated with 5% milk or BSA in tris-buffered saline with 0.1% tween20 and were probed with the specified primary antibody and the appropriate peroxidase-conjugated (Abcam) or fluorescent antibody (Abcam and Licor, NE) secondary antibody. Chemiluminescent signal was developed using Super Signal West Femto substrate (Pierce, Rockford, IL). Images were acquired using a signal detection system (iBright 1500FL, Thermo) and quantified with iBright image analysis software.

Mitochondrial Translocation: HUVECs were used to determine the mitochondrial localization of p66Shc. Cells were washed with cold 1xPBS buffer and collected in 500ul MSE buffer (5 mM MOPS, 70 mM sucrose, 2 mM EGTA, 220 mM mannitol, pH 7.2). Maintaining the cell suspension at 4ºC, cells were homogenized using a smooth PTFE pestle in glass tube until 85 to 95 % of the cells were ruptured. Unbroken cells and nuclei were removed by centrifugation at 1000g for 5 min. Supernatant was collected and centrifuge at 5000g for 10 min to obtain the mitochondrial and cytosolic fractions. The mitochondrial pellet was further processed for protein lysate, as described under Immunoblotting).

***Ex vivo* adenoviral infections and Vascular reactivity:** Ad-LacZ or Ad-HA-SUMO2 adenoviral stocks at a final concentration of 2.5×10^7 pfu/ml in EGM2 media were added to each aortic ring and incubated at 37°C for 24h. Infected vessels were suspended between two wire stirrups (150 mm) in a four-chamber myograph system (DMT Instruments) in 6 ml Krebs-Ringer (95% O2-5% CO_2, pH 7.4, 37°C). All concentration-effect curves were performed on arterial rings beginning at their optimum resting tone. Endothelium-dependent and –independent relaxation was determined by generating dose-response curves to acetylcholine (ACh 10^{-9}-10^{-5} M) and sodium nitroprusside (SNP 10^{-9}-10^{-5} M), respectively on phenylephrine (PE10^{-6} M)-induced pre-contracted vessels. Vasorelaxation evoked by ACh and SNP was expressed as percent contraction with reference to phenylephrine (PE 10^{-6} M) and determined by calculating the percentage of inhibition to the pre-constricted tension.

Statistics: All data met assumptions of the statistical test and all statistical analyses were performed using GraphPad Prism 9 unless specified. Data represent the mean ± SEM of at least three independent assays. Significance of differences between two groups was determined using a two-tailed independent sample Student *t*-test. One-way ANOVA was used for comparing more than two groups and two-way ANOVA was used for comparing two variables simultaneously, with each test followed by multiple comparison analysis. Vascular reactivity data was analyzed by non-linear regression analysis (curve fit) and significance of differences was determined by comparing two curves for the fitting line. Results were considered significant if P values were $\leq$ 0.05.

Acknowledgements

S. Kumar was supported by NIH grant R01HL152132 and CFF pilot and feasibility grant 005803I223. Sequencing data presented herein were obtained at the Genomics Division of the Iowa Institute of Human Genetics, which is supported, in part, by the University of Iowa Carver College of Medicine. Viral Vectors were provided by the University of Iowa Viral Vector Core. Mass spectrometry was performed at Mass Spectrometry and Proteomics Core Facility, University of Nebraska. The University of Nebraska Medical Center Mass Spectrometry and Proteomics Core Facility is administrated through the Office of the Vice Chancellor for Research and supported by state funds from the Nebraska Research Initiative. The p66ShcK81R knockin mouse was generated at the University of Iowa Genome Editing Core Facility, supported in part by grants from the NIH and from the University of Iowa Carver College of Medicine. We wish to thank Norma Sinclair, Patricia Yarolem, Joanne Schwarting and Rongbin Guan for their technical expertise in generating transgenic mice. We gratefully acknowledge Kris Griener of the Design Center for language editing and Dr. Jennifer Y. Barr of the Scientific Editing and Research Communication Core at the University of Iowa Carver College of Medicine for critical reading of the manuscript and suggestions toward improving the clarity of the manuscript.

References

1 Ludmer, P. L. *et al.* Paradoxical vasoconstriction induced by acetylcholine in atherosclerotic coronary arteries. *N Engl J Med* **315**, 1046-1051, doi:10.1056/NEJM198610233151702 (1986).

2 Lundberg, J. O. & Weitzberg, E. Nitric oxide signaling in health and disease. *Cell* **185**, 2853-2878, doi:10.1016/j.cell.2022.06.010 (2022).

3 Dai, G. *et al.* Distinct endothelial phenotypes evoked by arterial waveforms derived from atherosclerosis-susceptible and -resistant regions of human vasculature. *Proc Natl Acad Sci U S A* **101**, 14871-14876, doi:10.1073/pnas.0406073101 (2004).

4 Chang, H. M. & Yeh, E. T. H. SUMO: From Bench to Bedside. *Physiol Rev* **100**, 1599-1619, doi:10.1152/physrev.00025.2019 (2020).

5 Heo, K. S. *et al.* Disturbed flow-activated p90RSK kinase accelerates atherosclerosis by inhibiting SENP2 function. *J Clin Invest* **125**, 1299-1310, doi:10.1172/JCI76453 (2015).

6 Heo, K. S. *et al.* De-SUMOylation enzyme of sentrin/SUMO-specific protease 2 regulates disturbed flow-induced SUMOylation of ERK5 and p53 that leads to endothelial dysfunction and atherosclerosis. *Circ Res* **112**, 911-923, doi:10.1161/CIRCRESAHA.111.300179 (2013).

7 Song, J., Durrin, L. K., Wilkinson, T. A., Krontiris, T. G. & Chen, Y. Identification of a SUMO-binding motif that recognizes SUMO-modified proteins. *Proc Natl Acad Sci U S A* **101**, 14373-14378, doi:10.1073/pnas.0403498101 (2004).

8 Impens, F., Radoshevich, L., Cossart, P. & Ribet, D. Mapping of SUMO sites and analysis of SUMOylation changes induced by external stimuli. *Proc Natl Acad Sci U S A* **111**, 12432-12437, doi:10.1073/pnas.1413825111 (2014).

9 Wang, L. *et al.* SUMO2 is essential while SUMO3 is dispensable for mouse embryonic development. *EMBO Rep* **15**, 878-885, doi:10.15252/embr.201438534 (2014).

10 Zhang, F. P. *et al.* Sumo-1 function is dispensable in normal mouse development. *Mol Cell Biol* **28**, 5381-5390, doi:10.1128/MCB.00651-08 (2008).

11 Kim, Y. R. *et al.* SUMO2 regulates vascular endothelial function and oxidative stress in mice. *Am J Physiol Heart Circ Physiol* **317**, H1292-H1300, doi:10.1152/ajpheart.00530.2019 (2019).

12 Pinton, P. *et al.* Protein kinase C beta and prolyl isomerase 1 regulate mitochondrial effects of the life-span determinant p66Shc. *Science* **315**, 659-663, doi:10.1126/science.1135380 (2007).

13 Khanday, F. A. *et al.* Rac1 leads to phosphorylation-dependent increase in stability of the p66shc adaptor protein: role in Rac1-induced oxidative stress. *Mol Biol Cell* **17**, 122-129, doi:10.1091/mbc.e05-06-0570 (2006).

14 Kumar, S. *et al.* Sirtuin1-regulated lysine acetylation of p66Shc governs diabetes-induced vascular oxidative stress and endothelial dysfunction. *Proc Natl Acad Sci U S A* **114**, 1714-1719, doi:10.1073/pnas.1614112114 (2017).

15 Pacini, S. *et al.* p66SHC promotes apoptosis and antagonizes mitogenic signaling in T cells. *Mol Cell Biol* **24**, 1747-1757, doi:10.1128/MCB.24.4.1747-1757.2004 (2004).

16 Rozakis-Adcock, M. *et al.* Association of the Shc and Grb2/Sem5 SH2-containing proteins is implicated in activation of the Ras pathway by tyrosine kinases. *Nature* **360**, 689-692, doi:10.1038/360689a0 (1992).

17 Gotoh, N., Tojo, A. & Shibuya, M. A novel pathway from phosphorylation of tyrosine residues 239/240 of Shc, contributing to suppress apoptosis by IL-3. *EMBO J* **15**, 6197-6204 (1996).

18 Kumar, S. P66Shc and vascular endothelial function. *Biosci Rep* **39**, doi:10.1042/BSR20182134 (2019).

19 Napoli, C. *et al.* Deletion of the p66Shc longevity gene reduces systemic and tissue oxidative stress, vascular cell apoptosis, and early atherogenesis in mice fed a high-fat diet. *Proc Natl Acad Sci U S A* **100**, 2112-2116, doi:10.1073/pnas.0336359100 (2003).

20 Camici, G. G. *et al.* Genetic deletion of p66(Shc) adaptor protein prevents hyperglycemia-induced endothelial dysfunction and oxidative stress. *Proc Natl Acad Sci U S A* **104**, 5217-5222, doi:10.1073/pnas.0609656104 (2007).

21 Hajjar, D. P. & Gotto, A. M., Jr. Biological relevance of inflammation and oxidative stress in the pathogenesis of arterial diseases. *Am J Pathol* **182**, 1474-1481, doi:10.1016/j.ajpath.2013.01.010 (2013).

22 Wright, K. D., Staruschenko, A. & Sorokin, A. Role of adaptor protein p66Shc in renal pathologies. *Am J Physiol Renal Physiol* **314**, F143-F153, doi:10.1152/ajprenal.00414.2017 (2018).

23 Giorgio, M. *et al.* Electron transfer between cytochrome c and p66Shc generates reactive oxygen species that trigger mitochondrial apoptosis. *Cell* **122**, 221-233, doi:10.1016/j.cell.2005.05.011 (2005).

24 Abe, J. I. *et al.* Coordination of Cellular Localization-Dependent Effects of Sumoylation in Regulating Cardiovascular and Neurological Diseases. *Adv Exp Med Biol* **963**, 337-358, doi:10.1007/978-3-319-50044-7_20 (2017).

25 Woo, C. H. *et al.* Extracellular signal-regulated kinase 5 SUMOylation antagonizes shear stress-induced antiinflammatory response and endothelial nitric oxide synthase expression in endothelial cells. *Circ Res* **102**, 538-545, doi:10.1161/CIRCRESAHA.107.156877 (2008).

26 Francia, P. *et al.* Deletion of p66shc gene protects against age-related endothelial dysfunction. *Circulation* **110**, 2889-2895, doi:10.1161/01.CIR.0000147731.24444.4D (2004).

27 Chang, E. & Abe, J. I. Kinase-SUMO networks in diabetes-mediated cardiovascular disease. *Metabolism* **65**, 623-633, doi:10.1016/j.metabol.2016.01.007 (2016).

28 Abe, J. & Berk, B. C. Novel mechanisms of endothelial mechanotransduction. *Arterioscler Thromb Vasc Biol* **34**, 2378-2386, doi:10.1161/ATVBAHA.114.303428 (2014).

29 Stankovic-Valentin, N. *et al.* An acetylation/deacetylation-SUMOylation switch through a phylogenetically conserved psiKXEP motif in the tumor suppressor HIC1 regulates transcriptional repression activity. *Mol Cell Biol* **27**, 2661-2675, doi:10.1128/MCB.01098-06 (2007).

30 Wu, S. Y. & Chiang, C. M. Crosstalk between sumoylation and acetylation regulates p53-dependent chromatin transcription and DNA binding. *EMBO J* **28**, 1246-1259, doi:10.1038/emboj.2009.83 (2009).

31 Wu, R. F. *et al.* p66(Shc) Couples Mechanical Signals to RhoA through Focal Adhesion Kinase-Dependent Recruitment of p115-RhoGEF and GEF-H1. *Mol Cell Biol* **36**, 2824-2837, doi:10.1128/MCB.00194-16 (2016).

32 Garcia-Mata, R., Boulter, E. & Burridge, K. The 'invisible hand': regulation of RHO GTPases by RHOGDIs. *Nat Rev Mol Cell Biol* **12**, 493-504, doi:10.1038/nrm3153 (2011).
33 Thebault, P. *et al.* The C-type lectin-like receptor CLEC-1, expressed by myeloid cells and endothelial cells, is up-regulated by immunoregulatory mediators and moderates T cell activation. *J Immunol* **183**, 3099-3108, doi:10.4049/jimmunol.0803767 (2009).
34 Lopes Pinheiro, M. A. *et al.* Internalization and presentation of myelin antigens by the brain endothelium guides antigen-specific T cell migration. *Elife* **5**, doi:10.7554/eLife.13149 (2016).
35 Cheng, J., Kang, X., Zhang, S. & Yeh, E. T. SUMO-specific protease 1 is essential for stabilization of HIF1alpha during hypoxia. *Cell* **131**, 584-595, doi:10.1016/j.cell.2007.08.045 (2007).
36 Gong, L., Kamitani, T., Fujise, K., Caskey, L. S. & Yeh, E. T. Preferential interaction of sentrin with a ubiquitin-conjugating enzyme, Ubc9. *J Biol Chem* **272**, 28198-28201, doi:10.1074/jbc.272.45.28198 (1997).
37 Yadav, R. P., Gakhar, L., Yu, L. & Artemyev, N. O. Unique structural features of the AIPL1-FKBP domain that support prenyl lipid binding and underlie protein malfunction in blindness. *Proc Natl Acad Sci U S A* **114**, E6536-E6545, doi:10.1073/pnas.1704782114 (2017).
38 Wang, T. *et al.* SENP1-Sirt3 Signaling Controls Mitochondrial Protein Acetylation and Metabolism. *Mol Cell* **75**, 823-834 e825, doi:10.1016/j.molcel.2019.06.008 (2019).
39 Chen, Y., Liu, K., Zhang, G., Cheng, J. & Tu, J. Monoclonal antibody-based systematic identification of SUMO1-modification sites reveals TFII-I SUMOylation is involved in tumor growth. *J Cell Physiol*, doi:10.1002/jcp.31080 (2023).

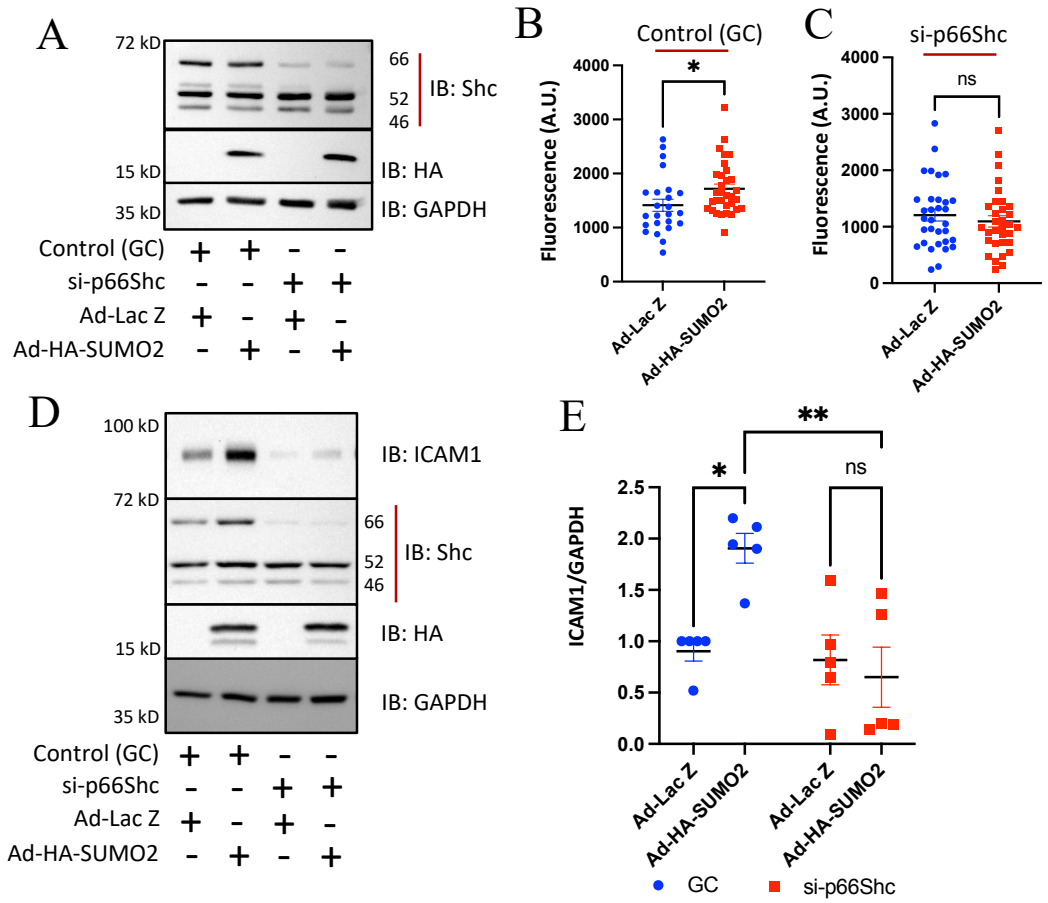

Figure 1: p66Shc mediates SUMO2-induced ROS production and inflammation in endothelial cells. (A) Immunoblot for Shc and SUMO2 expression in HUVECs following p66Shc knockdown (si-p66Shc) and SUMO2 overexpression (Ad-HA-SUMO2). (B and C) Quantification of ROS (MitoSOX fluorescence) in HUVECs from A. *P<0.05; n=24-32; student's t-test. (D) Immunoblot for ICAM1 expression following p66Shc knockdown (si-p66Shc) in HUVECs with and without SUMO2 overexpression (Ad-HA-SUMO2). (E) Quantification of ICAM1 from D. *<0.05, **P<0.01; n=3; one-way ANOVA. Data represents mean ±SEM. Immunoblots are representative of at least three independent experiments. GC, scrambled siRNA used as control; HUVECs, human umbilical vein endothelial cells; ICAM1, intercellular adhesion molecule 1.

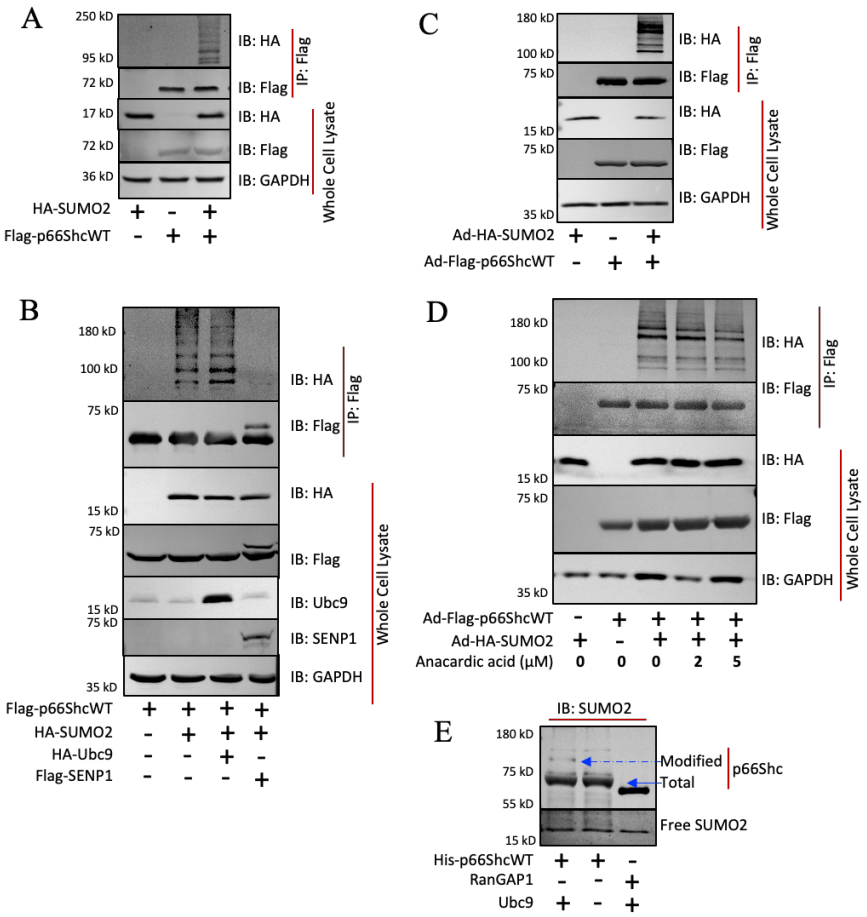

Figure 2: SUMO2 directly modifies p66Shc. (A) Immunoblot for sumoylated p66Shc in HEK-293 cells overexpressing SUMO2 (HA-SUMO2) and p66Shc (Flag-p66Shc). (B) Immunoblot for p66Shc sumoylation in HEK-293 cells overexpressing SUMO2 (HA-SUMO2) and p66Shc (Flag-p66Shc) with or without overexpression of Ubc9 (HA-Ubc9) and SENP1 (Flag-SENP1). (C) Immunoblot for sumoylation of p66Shc in HUVECs overexpressing SUMO2 (Ad-HA-SUMO2) or p66Shc (Ad-Flag-p66Shc). (D) Immunoblot for p66Shc sumoylation in HUVEC cells overexpressing SUMO2 (Ad-HA-SUMO2) or p66Shc (Ad-Flag-p66Shc) in the presence or absence of anacardic acid. (E) Immunoblot for sumoylated recombinant p66Shc in the presence of absence of Ubc9. Immunoblots are representative of at least three independent experiments.

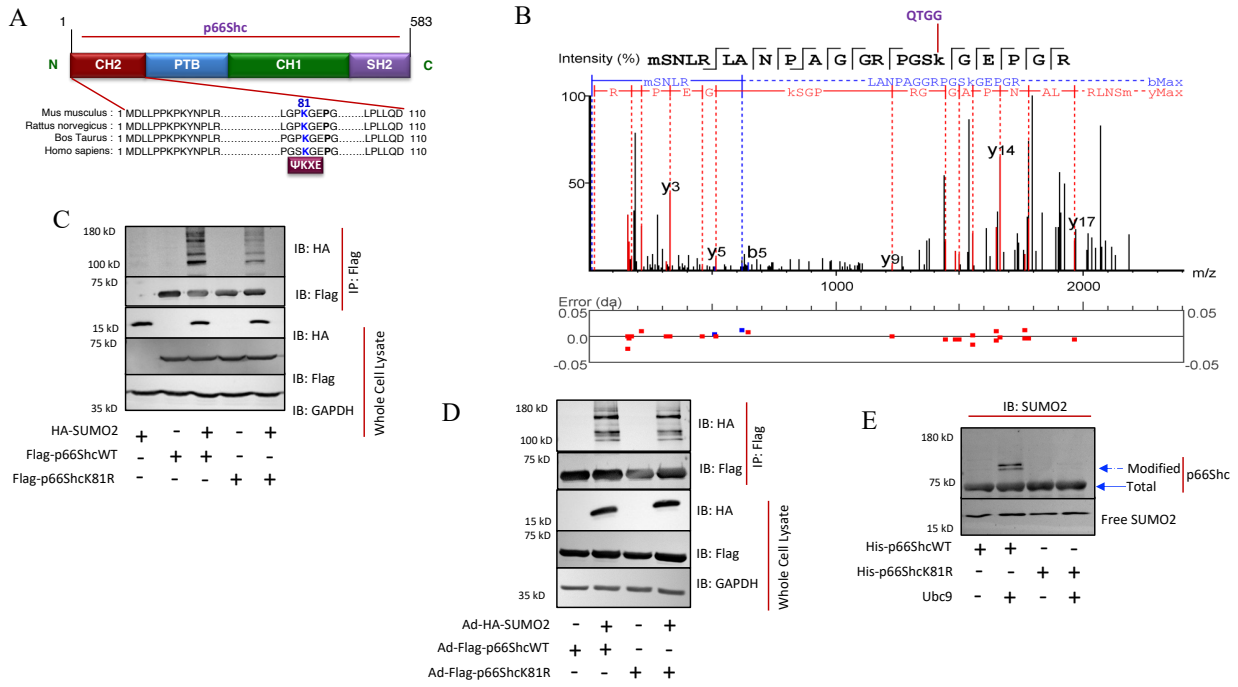

Figure 3: SUMO2 modifies p66Shc at lysine-81. (A) Modular structure of p66Shc showing conserved lysine-81 in the CH2 domain. (B) Tandem mass spectrometry of *in vitro SUMO*2ylated recombinant p66Shc. (C) Immunoblot showing sumoylation of p66Shc in HEK-293 cells overexpressing p66ShcWT (Flag-p66ShcWT) or p66ShcK81R (Flag-p66ShcK81R) with and without SUMO2 (HA-SUMO2). (D) Immunoblot showing sumoylation of p66Shc in HUVECs overexpressing p66ShcWT (Ad-Flag-p66ShcWT) or p66ShcK81R (Ad-p66ShcK81R) with and without SUMO2 (Ad-HA-SUMO2). (E) Immunoblot for sumoylation of recombinant p66ShcWT or p66ShcK81R. Immunoblots are representative of at least three independent experiments. CH2, collagen homology 2; PTB, phosphotyrosine binding; CH1, Collagen homology 1; SH2, Src homology 2.

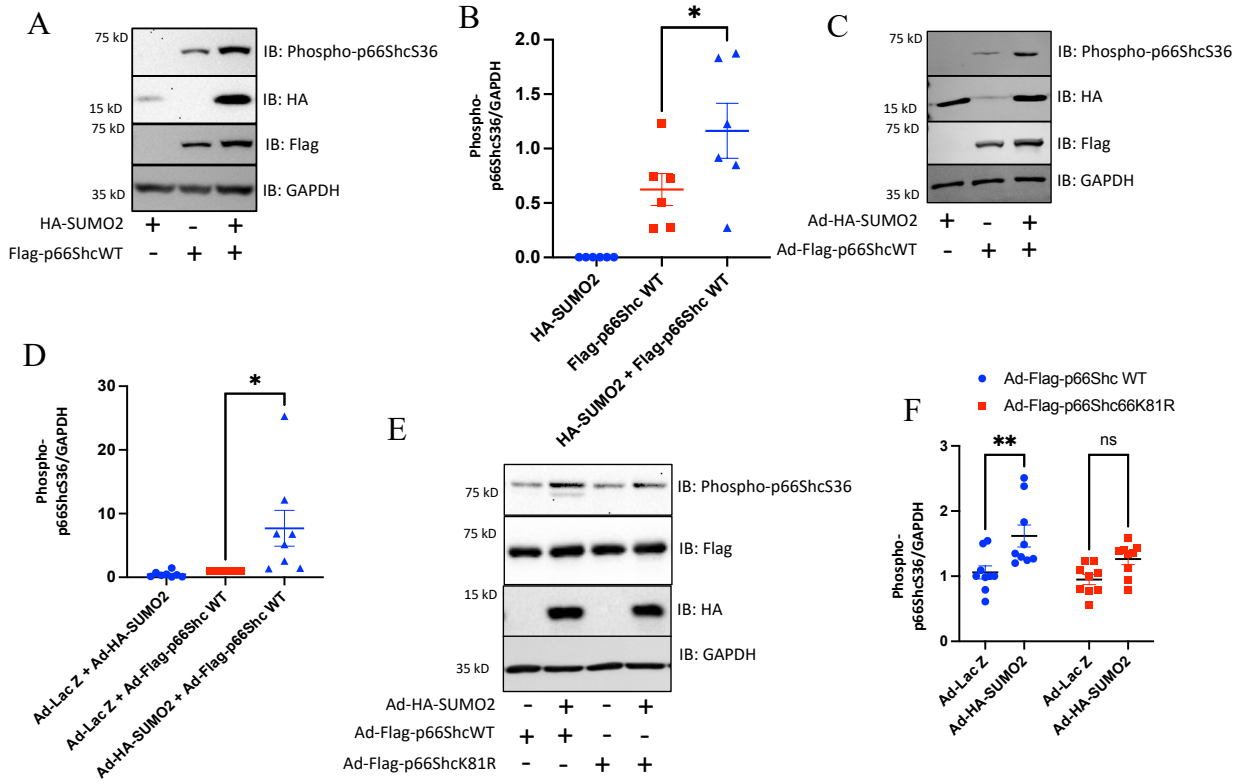

Figure 4: SUMO2 promotes p66ShcS36 phosphorylation by sumoylation of K81. (A) Immunoblot for p66ShcS36 phosphorylation in HEK-293 cells overexpressing SUMO2 (HA-SUMO2) and p66ShcWT (Flag-p66ShcWT). (B) Quantification of p66ShcS36 phosphorylation from A. *P<0.05; n=6; one-way ANOVA. (C) Immunoblot for p66ShcS36 phosphorylation in HUVECs overexpressing SUMO2 (Ad-HA-SUMO2) or p66ShcWT (Ad-Flag-p66ShcWT). (D) Quantification of p66ShcS36 phosphorylation from C. *P<0.05; n=8; one-way ANOVA. (E) Immunoblot for p66ShcS36 phosphorylation in HUVECs expressing SUMO2 (Ad-HA-SUMO2) and p66ShcWT (Ad-Flag-p66ShcWT) or p66ShcK81R (Ad-Flag-p66ShcK81R). (F) Quantification of p66ShcS36 phosphorylation from E. **P<0.01; n=6; two-way ANOVA. Immunoblots were quantified with iBright image analysis software. Data represents mean ±SEM. Immunoblots are representative of at least three independent experiments.

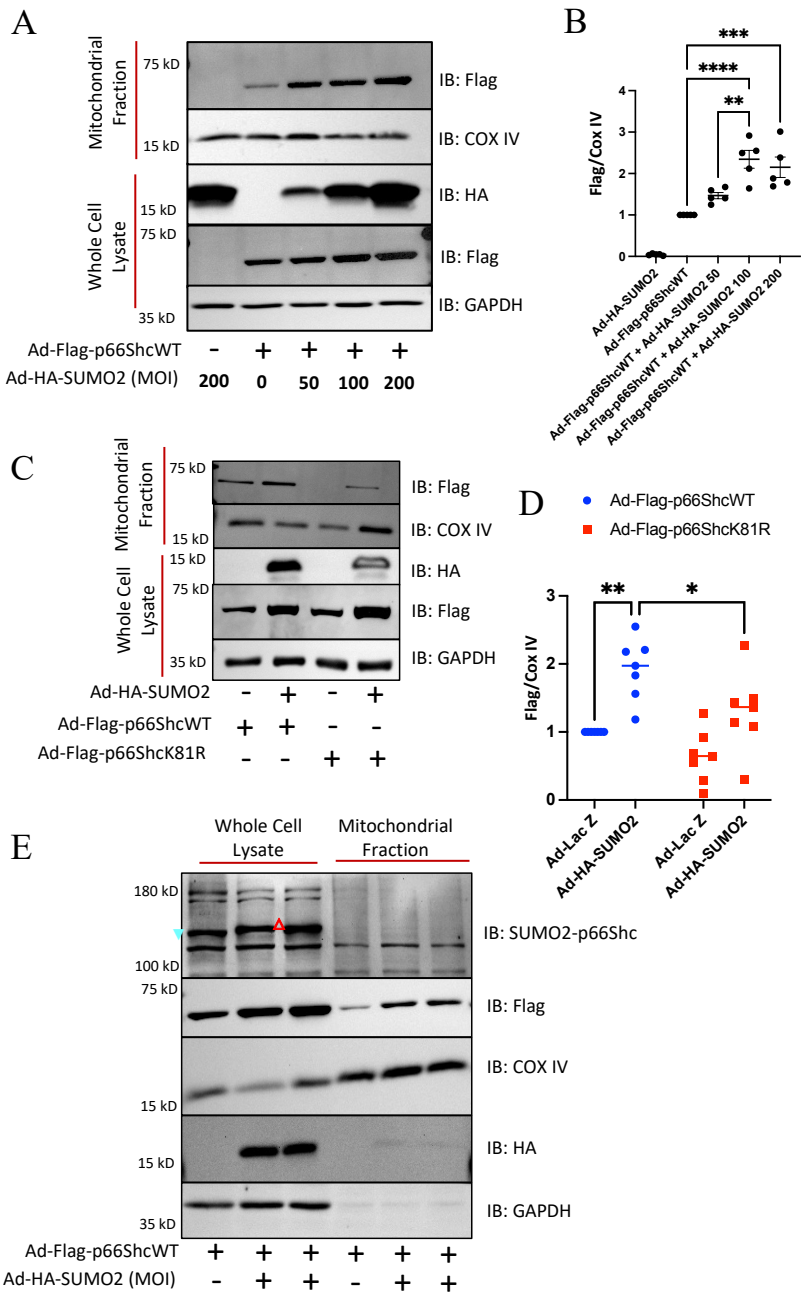

Figure 5: p66ShcK81 SUMO2ylation of K81 in p66Shc promotes its translocation to the mitochondria. (A) Immunoblot for p66ShcWT in whole cell lysates or the mitochondrial fraction of HUVECs ectopically expressing SUMO2 (Ad-HA-SUMO2) and p66ShcWT (Ad-Flag-p66ShcWT). (B) Quantification of the relative abundance of p66Shc in the mitochondria from A. **P<0.01, ****P<0.0001; n=5; one-way ANOVA. (C) Immunoblot for p66Shc in whole cell lysates or the mitochondrial fraction of HUVECs ectopically expressing SUMO2 (Ad-HA-SUMO2) and p66ShcWT (Ad-Flag-p66ShcWT or p66ShcK81R (Ad-Flag-p66ShcK81R). (D) Quantification of relative abundance of p66Shc in the mitochondria from C. *P<0.05, **P<0.01; n=7; two-way ANOVA. (E) Immunoblot for SUMO2ylated p66Shc (SUMO2-p66Shc) in whole

cell lysates and the mitochondrial fraction of HUVECs ectopically expressing SUMO2 (Ad-HA-SUMO2) and p66ShcWT (Ad-Flag-p66ShcWT). Cox IV was used as mitochondrial marker. Data represents mean ±SEM. Immunoblots are representative of at least three independent experiments. ▼-Non-specific band, ∆-SUMO2-p66Shc.

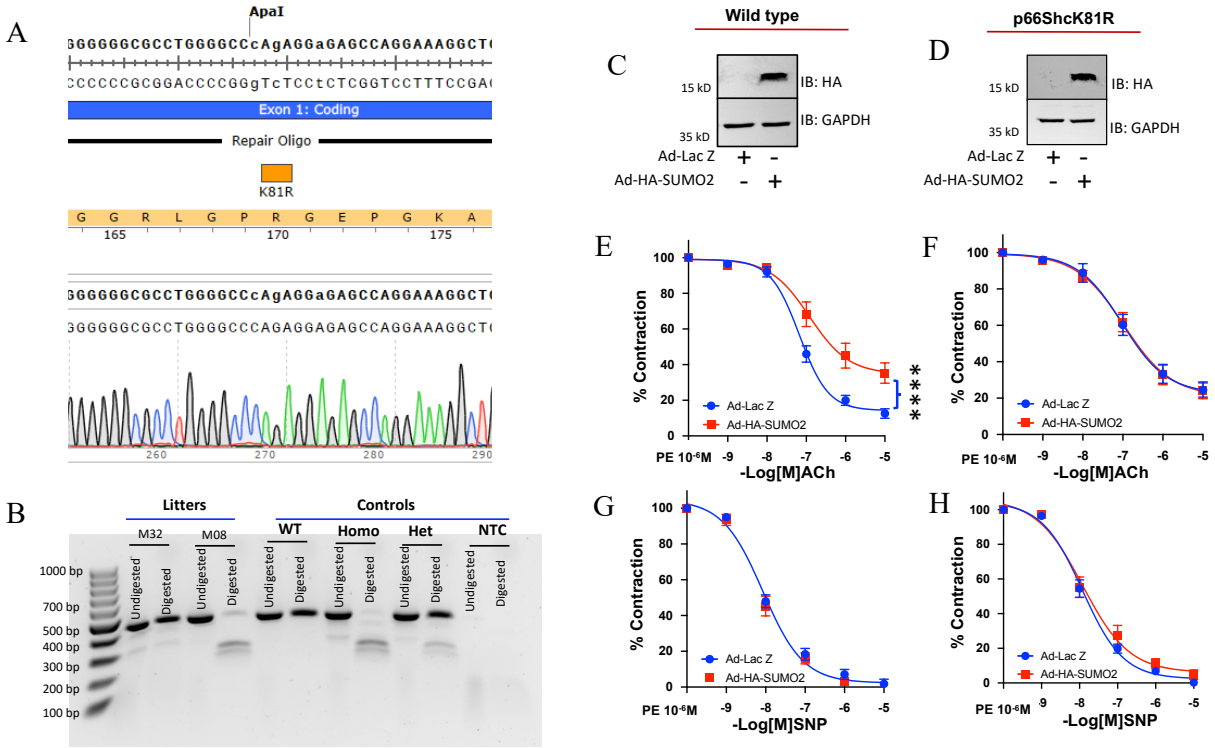

Figure 6: p66ShcK81R knockin (KI) are resistant to SUMO2-induced endothelial dysfunction. (A) DNA sequencing data from a p66ShcK81R knockin (KI) mouse showing a point mutation (A>G) resulting in an amino acid change (K→R), and insertion of silent mutation to create a digestion site for ApaI endonuclease for genotyping. (B) DNA gel electrophoresis of a PCR-amplified and ApaI-digested amplicon identifying the p66ShcK81R KI allele. (C and D) Representative immunoblots showing SUMO2 expression in aortic rings from wild type and p66ShcK81R KI mice ($1.67X10^8$ pfu/ring). (E and F) Graphs showing % contraction following induction of endothelium-dependent relaxation in aortic rings from (E) wild-type mice, n=14-16 from 4 mice) and (F) p66ShcK81R KI mice (n=15-16 rings from 4 mice) expressing a control vector (Ad-Lac Z) or overexpressing SUMO2 (Ad-HA-SUMO2). (G and H) Graphs showing % contraction following induction of endothelium-independent relaxation in aortic rings from (G) wild type (n=14-16 from 4 mice) and (H) p66ShcK81R KI mice (n=14-15 from 4 mice) expressing a control vector (Ad-Lac Z) or overexpressing SUMO2 (Ad-HA-SUMO2). Curves were compared for nonlinear fit. ****P<0.0001. Ach-acetylcholine, SNP-sodium nitroprusside, PE-Phenylephrine, Homo-homozygous, Het- heterozygous, and NTC- No template control. Data represents mean ±SEM.

Figure 7. SUMO2-p66Shc induced changes in endothelial cells are rescued by p66ShcK81R. Schematic presentation of key regulatory pathways impacted by SUMO2-p66Shc in endothelial cells, rescued by p66ShcK81R. Ingenuity Pathway Analysis (IPA) was performed on relative protein expression data from HUVECs expressing SUMO2 with p66ShcWT (top) or p66ShcK81R (bottom) compared to those expressing Ad-Lac Z. The figure illustrates the significant reversal observed in key regulatory pathways between p66ShcWT and p66ShcK81R conditions. Data are derived from a sample size of n=6.